Molecular Dynamics Analysis of NMR Relaxation in a Zinc-Finger Peptide

Arthur G. Palmer, III, and David A. Case*

Contribution from the Department of Molecular Biology, The Scripps Research Institute, La Jolla, California 92037. Received April 2, 1992

Abstract: The dynamical behavior of the 25-residue "zinc-finger" peptide xfin31 has been modeled through molecular dynamics simulations in vacuum and in water, and by normal mode and by Langevin mode analyses. The effects of internal motion on dipolar nuclear magnetic relaxation of C–H, N–H, and H–H spin pairs have been calculated, and the results for C–H pairs are compared to experimental results. Calculated internal correlation functions for directly bonded C–H and N–H spin pairs and for H–H spin pairs show rapid, subpicosecond initial decays followed by slower transitions to nearly constant "plateau" values. The fast initial decay contains underdamped oscillations in the gas-phase analysis and in the molecular dynamics simulations but is overdamped in the Langevin analysis. Quantum effects (estimated from the normal mode results) reduce the correlation functions at early times by about 0.05 for directly bonded C–H and N–H pairs and by less than 0.01 for H–H spin pairs. Correction factors relating cross-relaxation rate constants for inter-residue H–H spin pairs in rigid and nonrigid molecular models display a reasonably narrow distribution with an average value near 1. Calculated order parameters from solvated molecular dynamics simulations are in good agreement with experiment at most carbon positions. Implications of the results for the interpretation of "model-free" analyses of NMR relaxation rate constants and for NMR-based structural refinements are discussed.

I. Introduction

Many features of the general relation between molecular motion and NMR relaxation are well-understood,[1,2] but only in the past few years have systematic measurements on proteins become available that allow comparisons between observed and calculated behavior at many sites in the same molecule. In 1988 Wagner and co-workers reported ^{13}C spin–lattice relaxation parameters for the α carbons in BPTI;[3] subsequently, relaxation parameters, generally including spin–lattice and spin–spin relaxation rate or time constants and steady-state nuclear Overhauser enhancements, have been measured for ^{13}C–H and ^{15}N–H spin pairs in several polypeptides and proteins.[4–14]

Explorations of the connections between models of internal motion and relaxation parameters have been made for many years.[1,15–19] Experimental relaxation parameters determined for

proteins most often have been interpreted using the "model-free" formalism proposed by Lipari and Szabo,[20] although extensions to the basic formalism also have been used,[21] and alternative analytical procedures have been proposed.[22] The use of molecular dynamics simulations for interpretation of NMR relaxation parameters began shortly after such simulations on proteins became feasible,[19,23–26] but only recently have systematic solvated simulations become accessible. Since the character of internal motions as well as the nature of the average structure can be significantly affected by solvation, comparisons between solvated simulations and experiment permit new evaluations of the accuracy of the simulations and enable detailed interpretations of molecular motions leading to relaxation.

In the present work, solvated and vacuum molecular dynamics simulations and normal mode and Langevin mode calculations for a "zinc-finger" peptide are analyzed, and the results are compared to recent experimental investigations of ^{13}C NMR relaxation for backbone and side chain C–H spin pairs in the peptide.[7,27] The simulations also address the effects of internal motion on a set of 234 interresidue proton-proton NOESY cross-peaks that were used to determine a solution structure for the peptide.

II. Methods

The simulations were carried out on the 25-residue zinc-finger peptide xfin31 (see Figure 1),[7,28] using the AMBER 4 suite of programs[29] with the all-atom force field[30] and a TIP3 description

(1) London, R. E. *Meth. Enzymol.* **1989**, *176*, 358–375.

(2) Abragam, A. *Principles of Nuclear Magnetism*; Clarendon Press: Oxford, 1961.

(3) Nirmala, N. R.; Wagner, G. *J. Am. Chem. Soc.* **1988**, *110*, 7557–7558.

(4) Dellwo, M. J.; Wand, A. J. *J. Am. Chem. Soc.* **1989**, *111*, 4571–4578.

(5) Kay, L. E.; Torchia, D. A.; Bax, A. *Biochemistry* **1989**, *28*, 8972–8979.

(6) Clore, G. M.; Driscoll, P. C.; Wingfield, P. T.; Gronenborn, A. M. *Biochemistry* **1990**, *29*, 7387–7401.

(7) Palmer, A. G.; Rance, M.; Wright, P. E. *J. Am. Chem. Soc.* **1991**, *113*, 4371–4380.

(8) Kördel, J.; Skelton, N. J.; Akke, M.; Palmer, A. G., III; Chazin, W. J. *Biochemistry* **1992**, *31*, 4856–4866.

(9) Stone, M. J.; Fairbrother, W. J.; Palmer, A. G., III; Reizer, J.; Saier, M. H., Jr.; Wright, P. E. *Biochemistry* **1992**, *31*, 4394–4406.

(10) Kelsh, L. P.; Ellena, J. F.; Cafiso, D. S. *Biochemistry* **1992**, *31*, 5136–5144.

(11) Schneider, D. M.; Dellwo, M. J.; Wand, A. J. *Biochemistry* **1992**, *31*, 3645–3652.

(12) Takahashi, H.; Suzuki, E.; Shimada, I.; Arata, Y. *Biochemistry* **1992**, *31*, 2464–2468.

(13) Nicholson, L. K.; Kay, L. E.; Baldisseri, D. M.; Arango, J.; Young, P. E.; Bax, A.; Torchia, D. A. *Biochemistry* **1992**, *31*, 5253–5263.

(14) Barbato, G.; Ikura, M.; Kay, L. E.; Pastor, R. W.; Bax, A. *Biochemistry* **1992**, *31*, 5269–5278.

(15) Heatley, F. In *Annual Reports on NMR Spectroscopy*; G. A. Webb, Ed.; Academic: San Diego, 1986, pp 179–230.

(16) Wallach, D. *J. Chem. Phys.* **1967**, *47*, 5258–5268.

(17) Woessner, D. E. *J. Chem. Phys.* **1965**, *42*, 1855–1859.

(18) Tropp, J. *J. Chem. Phys.* **1980**, *72*, 6035–6043.

(19) Levy, R. M.; Karplus, M.; Wolynes, P. G. *J. Am. Chem. Soc.* **1981**, *103*, 5998–6011.

(20) Lipari, G.; Szabo, A. *J. Am. Chem. Soc.* **1982**, *104*, 4546–4559.

(21) Clore, G. M.; Szabo, A.; Bax, A.; Kay, L. E.; Driscoll, P. C.; Gronenborn, A. M. *J. Am. Chem. Soc.* **1990**, *112*, 4989–4991.

(22) Peng, J. W.; Wagner, G. *J. Magn. Reson.* **1992**, *98*, 308–332.

(23) Lipari, G.; Szabo, A.; Levy, R. M. *Nature* **1982**, *300*, 197–198.

(24) Olejniczak, E. T.; Dobson, C. M.; Karplus, M.; Levy, R. M. *J. Am. Chem. Soc.* **1984**, *106*, 1923–1930.

(25) Levy, R. M.; Dobson, C. M.; Karplus, M. *Biophys. J.* **1982**, *39*, 107–113.

(26) Kessler, H.; Griesinger, C.; Lautz, J.; Müller, A.; van Gunsteren, W. F.; Berendsen, H. J. C. *J. Am. Chem. Soc.* **1988**, *110*, 3393–3396.

(27) Palmer, A. G.; Hochstrasser, R.; Millar, D. P.; Rance, M.; Wright, P. E. Submitted for publication.

(28) Lee, M. S.; Gippert, G. P.; Soman, K. V.; Case, D. A.; Wright, P. E. *Science* **1989**, *245*, 635–637.

(29) Pearlman, D. A.; Case, D. A.; Caldwell, J. C.; Seibel, G. L.; Singh, U. C.; Weiner, P.; Kollman, P. A. *AMBER 4.0*; University of California: San Francisco, 1991.

(30) Weiner, S. J.; Kollman, P. A.; Nguyen, D. T.; Case, D. A. *J. Comput. Chem.* **1986**, *7*, 230–252.
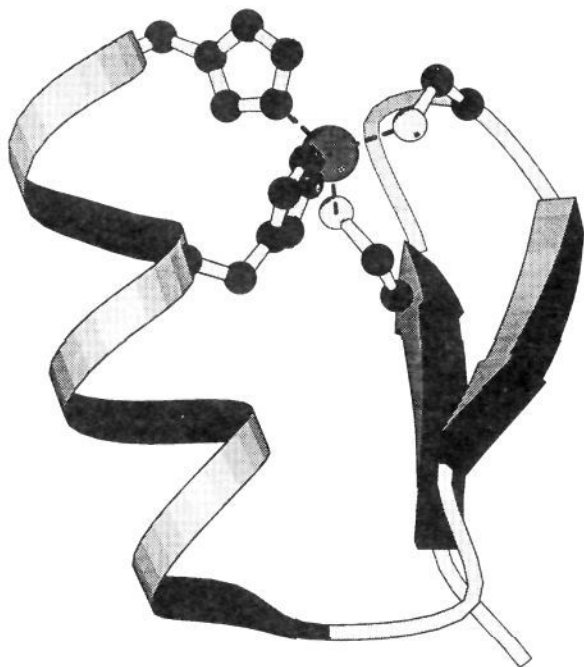
Figure 1. Structure of xfin32 zinc-finger peptide. Shown is a ribbon diagram of the structure of the peptide determined by NMR spectroscopy.

for water.[31]   Parameters for the zinc coordination have been described earlier[32] and were based on EXAFS data on a zinc finger[33] and on X-ray data from other zinc–peptide complexes.[34] Figure 1 shows a cartoon of the structure, which has a short stretch of antiparallel β sheet near the N-terminus and a helix spanning most of the C-terminal half of the molecule. As the figure indicates, these two pieces of secondary structure are connected by a short loop at the bottom (comprising residues Val 11 to Lys 13) and by zinc coordination at the top. These connections appear to give the domain a native structure like those found in globular proteins; there is no evidence for major conformational heterogeneity.[28]

Harmonic Calculations. Our starting conformation was the NMR-refined structure with the lowest total energy determined from a recent calculation that used the methodology described earlier[28,32] but with a considerably larger set of NMR-based distance and angle restraints; details will be published separately. For the normal modes calculations, this structure was energy-minimized using a conjugate gradient procedure (without NMR-related penalty functions) until the root-mean-square (rms) of the elements of the gradient matrix was less than 10^{-5} kcal/(Å mol). The rms deviation of the backbone heavy atoms (N, Cα, C, and O) between the minimized and NMR-refined structures was 0.74 Å, and all of the hydrogen bonds present in the NMR structure were maintained in the minimized structure. Gas-phase normal modes were computed in the usual way by constructing and diagonalizing a mass-weighted matrix of second derivatives in Cartesian space.[35-37] The two lowest normal mode frequencies were 8.1 and 9.7 cm^{-1}; an additional 10 modes had frequencies below 20 cm^{-1}, and 12 more modes had frequencies below 30 cm^{-1}.

These distributions are similar to those described earlier for other small proteins.[38] Langevin modes, which solve the same problem in the presence of a viscous continuum solvent and a white-noise random force,[39] were computed as described earlier,[40] with a solvent viscosity of 0.9 cp. A total of 216 overdamped modes were observed, which approximately corresponds to all gas-phase normal modes with frequencies below 100 cm^{-1} becoming overdamped in the Langevin analysis; again, the distributions of damping times and frequencies are similar to those reported earlier for other small proteins[40] and are not given here. For a given potential, the *magnitudes* of fluctuations from the minimum-energy structure are independent of the assumed solvent viscosity, but the *rates* of decay of such fluctuations do depend upon this parameter.

NMR spin relaxation mediated by the dipolar coupling between two spins depends upon the motions in the laboratory reference frame of a vector connecting the two spins. In the present work, internal and overall motions of the peptide are assumed to be statistically independent (or timescale separated); therefore, a correlation function for motions of $\mathbf{r}(t)$ can be expressed as the product of a correlation function for overall rotational diffusion and a correlation function for internal motions in a fixed molecular frame of reference. For two spins at a fixed distance, the internal angular correlation function that governs NMR spin relaxation is given by

$$C(\tau) = \langle P_2[\hat{\mu}(0)\cdot\hat{\mu}(\tau)]\rangle \tag{1}$$

in which $\hat{\mu}(\tau)$ is a unit vector in the direction of the vector $\mathbf{r}(t)$ connecting the spins at time t in the molecular reference frame, and $\langle\ \rangle$ indicates an ensemble average. The correlation functions were calculated from the normal and Langevin modes using a Taylor series expansion[39,41] that expresses the correlation functions in terms of the mean-square deviations of the cartesian coordinates from their equilibrium positions. For a classical system connected to a heat bath of temperature T, these fluctuations are given by[42]

$$\langle q_i(0)q_j(\tau)\rangle = \delta_{ij}\frac{kT}{\omega^2}\cos(\omega\tau) \tag{2}$$

in which q_i is the mass-weighted deviation of the ith coordinate from its equilibrium position in a mode with frequency ω. For Langevin modes, the frequency may be complex, which leads to damped oscillatory decay. For quantum statistics, on the other hand,[42]

$$\langle q_i(0)q_j(\tau)\rangle = \delta_{ij}(\hbar/2\omega)\coth(\hbar\omega/2kT)\cos(\omega\tau) \tag{3}$$

In the present case, the most important consequence of this change is that fluctuations arising from modes of high frequencies never drop below their zero-point values. As shown below, zero-point motion effects can be significant for some types of relaxation behavior.

Molecular Dynamics. The solvated molecular dynamics simulations were performed using periodic boundary conditions, a temperature of 300 K, and a pressure of 1 atm. A time step of 1 fs was used for integrating Newton's equations and nonbonded forces were truncated at a distance of 12 Å. Temperature and pressure were regulated using a weakly coupled bath[43] with relaxation parameters of 0.1 and 1.0 ps, respectively. The starting conformation was the NMR-refined structure described above. The peptide was embedded in a 50-Å × 45-Å × 37-Å box containing 2693 water molecules chosen to allow a shell of approximately 9 Å around the solute. The energy of the system was minimized using a conjugate gradient algorithm, and the dynamics steps heated the system to 300 K followed by 25 ps of equilibration

(31) Jorgensen, W. L. *J. Chem. Phys.* **1982**, *77*, 4156.
(32) Lee, M. S.; Gippert, G. P.; Soman, K. V.; Case, D. A.; Wright, P. E. In *Structure & Methods, Volume 2: DNA Protein Complexes & Proteins*; Sarma, R. H.; Sarma, M. H., Eds.; Adenine Press: Albany, NY, 1990, pp 83–91.
(33) Diakun, G. P.; Fairall, L.; Klug, A. *Nature* **1986**, *324*, 698.
(34) Freeman, H. C. In *Inorganic Biochemistry*; Eichorn, G. L., Ed.; Elsevier: Amsterdam, 1973, pp 121–166.
(35) Brooks, B.; Karplus, M. *Proc. Natl. Acad. Sci. U.S.A.* **1983**, *80*, 6571–6575.
(36) Go, N.; Noguti, T.; Nishikawa, T. *Proc. Natl. Acad. Sci. U.S.A.* **1983**, *80*, 3696–3700.
(37) Levitt, M.; Sander, C.; Stern, P. S. *J. Mol. Biol.* **1985**, *181*, 423–447.

(38) Teeter, M. M.; Case, D. A. *J. Phys. Chem.* **1990**, *94*, 8091–8097.
(39) Lamm, G.; Szabo, A. *J. Chem. Phys.* **1986**, *85*, 7334–7348.
(40) Kottalam, J.; Case, D. A. *Biopolymers* **1990**, *29*, 1409–1421.
(41) Henry, E. R.; Szabo, A. *J. Chem. Phys.* **1985**, *82*, 4753–4761.
(42) McQuarrie, D. A. *Statistical Mechanics*; Harper and Row: New York, 1976.
(43) Berendsen, H. J. C.; Postma, J. P. M.; van Gunsteren, W. F.; DiNola, A.; Haak, J. R. *J. Chem. Phys.* **1984**, *81*, 3684–3690.

NMR Relaxation in a Zinc-Finger Peptide

J. Am. Chem. Soc., Vol. 114, No. 23, 1992 9061

and 100 ps of data collection. Coordinates were saved at 0.1-ps intervals during the trajectory. The rms deviation of the backbone heavy atoms (N, Cα, C, and O) between the NMR-refined structure and the equilibrated structure at the beginning of the 100-ps trajectory was 0.34 Å. All of the hydrogen bonds present in the NMR structure were maintained in the equilibrated structure.

For comparative purposes, a second simulation was run with the same general procedure but in a smaller box with 1653 waters; this trajectory was recorded for 125 ps. To examine the subpicosecond behavior of the correlation functions, coordinates were recorded at 0.002-ps intervals for a 5-ps section in the middle of the second simulation. The molecular dynamics simulation in vacuo was performed in a similar fashion except that no periodic boundary conditions or pressure regulations were involved, a distance-dependent dielectric with $\epsilon = r$ in angstroms was used,[30] and data were recorded for 350 ps. The rms deviation of the backbone heavy atoms between the NMR-refined structure and the equilibrated structure at the beginning of the trajectory was 1.51 Å; as discussed below, the hydrogen-bonding pattern differed between the solvated and vacuum simulations, so only qualitative comparisons should be made between them.

Prior to calculation of the correlation functions, overall motion of the molecule was removed by rotating the coordinate sets to superimpose the instantaneous principal axis frames of reference. In practice, the characteristic times over which the correlation funtions have been calculated are short relative to the characteristic time for overall motion; consequently, the procedure by which the overall motion is removed from the molecule is not critical, and nearly identical correlation functions were obtained for calculations in which coordinate sets were superimposed by using a least-squares fit of all atoms[44] or in which no attempt was made to remove overall rotation.

The total internal correlation function for dipolar spin relaxation, including the effects of both angular and radial fluctuations, is given by the following generalization of eq 1

$$C(\tau) = c\langle P_2[\hat{\mu}(0)\cdot\hat{\mu}(\tau)]/[r(0)r(\tau)]^3\rangle \qquad (4)$$

in which c is a normalization constant. In the present work, we chose $c = \langle r^{-6}\rangle^{-1}$, which ensures that $C(0) = 1$ and facilitates comparison with experimental results. Equation 4 cannot be directly applied in the calculation of correlation functions for spins that are related by symmetry operations. For example, the correlation functions for methyl C–H spin pairs and phenyl δ spin pairs are determined by averaging the correlation functions calculated separately for each of the symmetry-related C–H spin pairs using eq 4. Similar complications arise in the calculation of correlation functions for H–H spin pairs when one or both of the H spins are methyl protons. In the present work, correlation functions for H–H pairs in which either of the spins were methyl protons have not been determined; models for the effects of methyl rotation on the dipolar relaxation of protons have been discussed elsewhere.[45,46]

Order Parameters and Effective Correlation Times. The square of the order parameter, S^2, is defined as

$$S^2 = \lim_{\tau\to\tau_c} C(\tau) \qquad (5)$$

in which $C(\tau)$ is given by eq 1 or 4 and τ_c is an intermediate time, much less than the overall rotation time, by which $C(\tau)$ becomes constant. The existence of such a plateau assumes that the internal correlation function decays to its limiting value on a timescale short compared to overall rotation; this assumption is examined below. The definitions of the normalization constant in eq 4 and the order parameter in eq 5 are analogous to the definitions in the Lipari–Szabo model-free internal correlation function[20]

(44) McLachlan, A. D. *J. Mol. Biol.* **1979**, *128*, 49–79.
(45) Olejniczak, E. T. *J. Magn. Reson.* **1989**, *81*, 392–394.
(46) Yip, P.; Case, D. A. In *Computational Aspects of the Study of Biological Macromolecules by NMR Spectroscopy*; Hoch, J., Ed.; Plenum: New York, 1991. pp 317–330.

$$C_{MF}(\tau) = \langle r^{-6}\rangle \{S^2_{MF} + (1 - S^2_{MF})\exp(-\tau/\tau_e)\} \qquad (6)$$

in which the square of the order parameter, S^2_{MF}, and the effective internal correlation time, τ_e, are obtained by analysis of experimental data. For convenience, S^2 and S^2_{MF} will be referred to simply as order parameters.

In most cases, approximate plateaus in the correlation functions calculated from eqs 1 and 4 were reached by 20 ps, and the order parameters were estimated as

$$S^2 = \int_{19.5}^{20.5} C(\tau)\,d\tau \qquad (7)$$

with $C(\tau)$ given by eqs 1 or 4. Correlation functions calculated from the Langevin mode analysis (eq 1) reached plateaus in much less than 20 ps; consequently, values of S^2 calculated using eq 7 were equivalent to instantaneous values of $C(\tau)$ at 20 ps. The effective internal correlation times, τ_e, were calculated as[20]

$$\tau_e = (1 - S^2)^{-1}\int_0^{20}[C(\tau) - S^2]\,d\tau \qquad (8)$$

with S^2 defined as in eq 7. Order parameters can also be estimated by using the addition theorem for spherical harmonics to expand eq 4 together with the property that

$$\lim_{\tau\to\infty}\langle Y^2_m[\Omega(0)]Y^2_m[\Omega(\tau)]\rangle = \langle Y^2_m[\Omega(t)]\rangle^2 \qquad (9)$$

in which $\Omega(t)$ are the polar angles defining the orientation of $r(t)$. Using the above properties in eq 5 yields an asymptotic estimate of the order parameter:

$$S^2_a = c\sum_{m=-2}^{2}\langle Y^2_m[\Omega(t)]/r^3\rangle^2 \qquad (10)$$

For finite trajectories, $C(\tau)$ calculated using eq 4 will be subject to a statistical uncertainty that can be estimated as[47]

$$\Delta[C(\tau)] = C(\tau)[1 - C(\tau)](2\tau_e/t_{run})^{1/2} \qquad (11)$$

in which t_{run} is the length of the trajectory, and the analysis recognizes that the number of independent "samples" in the trajectory is determined by t_{run}/τ_e. In some cases, the decay of a correlation function is dominated by infrequent jumps between energy minima. If only a few such jumps are recorded in a particular trajectory, the simulations provide only qualitative information about the magnitudes of effective order parameters. This is discussed more fully below.

Simulation of the relaxation of methyl groups is complicated by the superposition of the rotational motion of the methyl group and the motion of the symmetry axis of the methyl group. If the motion of the protons about the 3-fold symmetry axis is uncorrelated with other motions, the order parameter for the C–H spin pair can be factored as[20]

$$S^2 = P_2(\cos\theta)^2S^2_0 = 0.1107S^2_0 \qquad (12)$$

in which $\theta = 70.5°$ is the angle between the symmetry axis and a C–H vector and S^2_0 is the order parameter of the symmetry axis. Thus, the order parameter for the C–H vector can be estimated from the correlation function for the C–C spin pair defining the symmetry axis of the methyl group as well as by direct calculation of the average correlation function for the three C–H spin pairs. Similar considerations are applicable to the correlation functions for H–H spin pairs when one or both of the H spins are methyl protons. Appropriate models for the effects of methyl rotation on the dipolar relaxation of protons have been described elsewhere.[45,46]

Proton NOESY Intensities. Determination of three-dimensional structures by NMR spectroscopy is possible because the rate constant for dipolar cross-relaxation between two protons depends strongly upon their separation. A complete description of magnetization transfer through a system of n protons requires the solution of n coupled differential equations; consequently, the cross-relaxation rate constant is related directly only to the initial

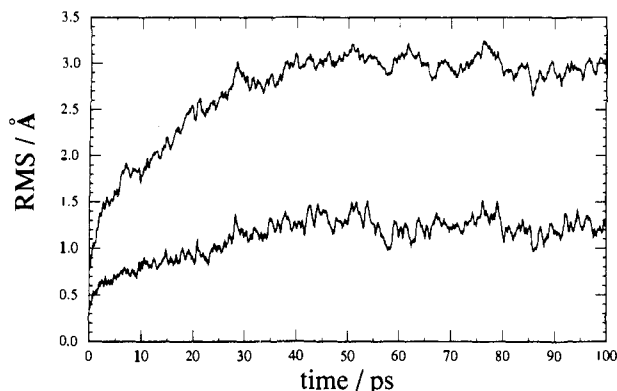(47) Zwanzig, R.; Ailawadi, N. K. *Phys. Rev.* **1969**, *182*, 280–283.

Figure 2. Root-mean-square (rms) deviations relative to the NMR structure of the xfin31 peptide. The lower and upper curves show the rms deviations for the backbone heavy atoms and all atoms, respectively.

rate of development of a cross-peak in a NOESY experiment. Proton NOESY cross-peak intensities frequently are interpreted assuming that the proton pairs are rigidly attached to the molecule, although considerable earlier work has addressed the effects of internal motions of the spin pairs.[24,48-50] For a macromolecule in the slow tumbling regime, the cross-relaxation rate is dominated by the spectral density at zero frequency, which is given by the integral of the correlation function for combined internal and overall motions. Assuming that overall motion can be described by isotropic rotational diffusion with a correlation function proportional to $\exp(-\tau/\tau_m)$ and that τ_e is much less than τ_m, the overall rotational tumbling time, the ratio of the cross-relaxation rate constants for mobile and rigid proton pairs approximately is given by

$$Q = \langle (\bar{r}/r)^6 \rangle S^2 \equiv RS^2 \tag{13}$$

in which $\bar{r}$ is the distance between the interacting proton spins in the rigid model and R measures the effects of radial fluctuations. Although the values of S^2 and R depend upon the choice of the normalization constant in eq 4, the product Q is independent of the particular normalization employed; the normalization $c = \langle r^{-3} \rangle^{-2}$ has been used elsewhere.[50] In the present work, $\bar{r}$ was chosen to be the average interproton distance calculated over the trajectory; thus, $0 \le S^2 \le 1$ and $R \ge 1$.

III. Results

A. General Features of the Simulation. The NMR structure of xfin31 (Figure 1) has hydrogen bonds between Tyr 1 NH and Phe 10 CO and between Phe 10 NH and Tyr 1 CO in the β region of the peptide; in addition, a series of backbone NH–CO hydrogen bonds characteristic of α and 3_{10} helices extend from residues 16–24.[32] All hydrogen bonds present in the NMR structure were maintained during the solvated MD simulations. The rms deviations between the heavy atoms in the NMR structure and the structures along the MD trajectory averaged 1.22 Å; the average rms deviations for all atoms was 2.87 Å. A graph of rms deviations along the trajectory is shown in Figure 2. The structure of the peptide in the vacuum simulation deviated more strongly from the NMR structure: the hydrogen bonds between Tyr 1 and Phe 10 were present only transiently during the trajectory, and a number of hydrogen bonds developed that were lacking in the NMR structure or in the solvated simulation. The average rms deviation between the heavy atoms and the NMR structure was 1.59 Å; for all atoms the average rms deviation was 2.98 Å. As discussed below, formation of incorrect hydrogen bonds in the vacuum simulation was correlated with distinct differences between the order parameters calculated from solvated and vacuum simulations; thus, solvated MD simulations appear necessary for

Table I. Order Parameters for N–H and C–H Spin Pairs[a]

residue	NH	C^α	C^β	C^γ	C^δ	C^ϵ	C^ζ
Tyr 1	0.74	0.88	0.84		0.71	0.69	
Lys 2	0.81	0.91	0.55	0.22	0.41	0.40	
Cys 3	0.84	0.85	0.81				
Gly 4	0.68	0.61					
Leu 5	0.73	0.92	0.81	0.26	0.38, 0.23		
Cys 6	0.62	0.90	0.88				
Glu 7	0.83	0.89	0.82	0.75			
Arg 8	0.79	0.84	0.77	0.68	0.73		
Ser 9	0.80	0.90	0.81				
Phe 10	0.79	0.91	0.80		0.70	0.68	0.75
Val 11	0.58	0.70	0.74	0.12, 0.38			
Glu 12	0.74	0.79	0.64	0.37			
Lys 13	0.76	0.82	0.47	0.37	0.31	0.28	
Ser 14	0.82	0.84	0.47				
Ala 15	0.79	0.89	0.57				
Leu 16	0.85	0.91	0.84	0.66	0.24, 0.18		
Ser 17	0.84	0.88	0.82				
Arg 18	0.83	0.89	0.50	0.07	0.16		
His 19	0.83	0.89	0.83		0.80	0.72	
Gln 20	0.83	0.89	0.81	0.50			
Arg 21	0.88	0.87	0.81	0.70	0.46		
Val 22	0.79	0.81	0.79	0.17, 0.18			
His 23	0.82	0.87	0.81		0.81	0.78	
Lys 24	0.77	0.78	0.75	0.66	0.57	0.28	
Asn 25	0.37	0.24	0.23				

[a] Order parameters were estimated from a 100-ps solvated MD simulation using eqs 4 and 7. Only the order parameters for the C–H1 spin pairs are reported for methylene groups; the order parameters for C–H2 spin pairs were similar. The mean absolute deviation between C–H1 and C–H2 order parameters was 0.05; the largest difference observed was 0.13 for Arg 8 C^δ spin pairs. The average uncertainties in the order parameters, calculated using eq 11 and the data in Tables I and III, are 0.04 for backbone N–H and C–H spin pairs and 0.06 for side chain C–H spin pairs.

realistic simulations of NMR relaxation, at least for this small protein.

Correlation functions calculated from the 100-ps solvated MD trajectory using eq 4 are shown in Figure 3 for the C–H and N–H spin pairs of Phe 10 and Leu 16. The correlation functions were characterized by a very rapid decay in the first few tenths of picoseconds; a slower decay was observed for times greater than 1 ps. Plateau were generally reached in the correlation functions by 20 ps for backbone spin pairs; the plateaus were less well defined for some C–H spin pairs of side chains. For example, the order parameters calculated using eqs 7 and 10 differed by more than 0.1 for only 2 of the 50 backbone C–H and N–H spin pairs but differed by this much for 15 of the 65 side chain C–H spin pairs.

The subpicosecond behavior of the correlation functions is illustrated in Figure 4 for the $C\alpha$–H spin pair of Ala 15: high frequency oscillations were observed for the MD simulations and for the normal mode analysis, but the oscillations were overdamped in the Langevin calculation. The period of oscillation in Figure 4 corresponds to a vibrational frequency of about 1100 cm^{-1} and suggests that bending modes in this frequency regime contribute to the correlation function decay at short times. The similarities between the short time behavior of the correlation functions calculated from the normal mode analysis and from the MD simulations suggest that the damping effect of viscosity was overestimated in the Langevin analysis. Similar behavior has been noted in earlier studies.[51]

B. C–H and N–H Spin Pairs. Values of the order parameters determined from the C–H and N–H correlation functions calculated using eq 7, the asymptotic values of the order parameters calculated using eq 10, and the effective correlation times calculated using eq 8 are given in Tables I–III for the 100-ps solvated MD simulation. Uncertainties in the order parameters shown in Table I were estimated using eq 11 to be 0.04 for backbone spin pairs and 0.06 for side chain spin pairs. As discussed below (cf. Table VIII), the differences between order parameters determined

(48) LeMaster, D. M.; Kay, L. E.; Brünger, A. T.; Prestegard, J. H. *FEBS Lett.* **1988**, *236*, 71–76.

(49) Brüschweiler, R.; Roux, B.; Blackledge, M.; Griesinger, C.; Karplus, M.; Ernst, R. R. *J. Am. Chem. Soc.* **1992**, *114*, 2289–2302.

(50) Post, C. B. *J. Mol. Biol.* **1992**, *224*, 1087–1101.

(51) Xiang, T.; Liu, F.; Grant, D. M. *J. Chem. Phys.* **1991**, *95*, 7576–7590.
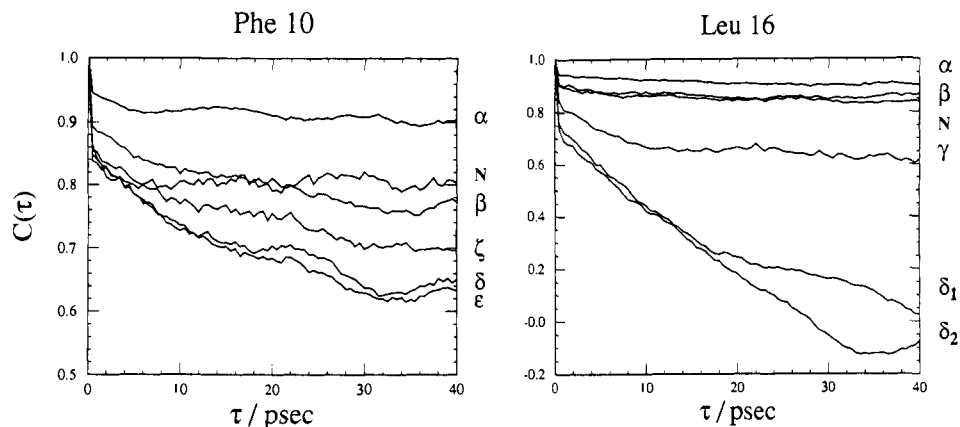
Figure 3. Correlation functions for C–H spin pairs of Phe 10 and Leu 16, calculated using eq 4. Correlation functions for Phe 10 δ, Phe 10 ϵ, Leu 16 δ_1, and Leu 16 δ_2 are the averages of the correlation functions for the symmetry-related C–H spin pairs.
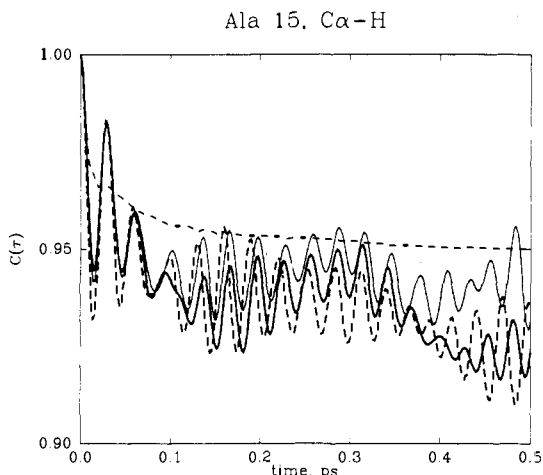

Figure 4. Short-time correlation functions for the C–H spin pair of Ala 15. The correlation functions were calculated from solvated MD (heavy solid curve), vacuum MD (light solid curve), gas-phase normal mode analysis (heavy dashed curve), and Langevin analysis (light dashed curve).

Table II. Asymptotic Order Parameters for N–H and C–H Spin Pairs[a]

residue	NH	C^α	C^β	C^γ	C^δ	C^ϵ	C^ζ
Tyr 1	0.69	0.87	0.83		0.69	0.68	
Lys 2	0.79	0.91	0.51	0.15	0.29	0.28	
Cys 3	0.83	0.86	0.81				
Gly 4	0.67	0.66					
Leu 5	0.72	0.92	0.82	0.29	0.40, 0.16		
Cys 6	0.61	0.87	0.88				
Glu 7	0.82	0.88	0.81	0.74			
Arg 8	0.79	0.85	0.78	0.70	0.77		
Ser 9	0.81	0.90	0.81				
Phe 10	0.79	0.91	0.80		0.71	0.70	0.74
Val 11	0.60	0.56	0.65	0.26, 0.23			
Glu 12	0.66	0.70	0.55	0.17			
Lys 13	0.75	0.79	0.37	0.28	0.23	0.21	
Ser 14	0.81	0.86	0.44				
Ala 15	0.79	0.88	0.28				
Leu 16	0.86	0.91	0.86	0.61	0.17, 0.19		
Ser 17	0.85	0.88	0.82				
Arg 18	0.85	0.90	0.26	0.15	0.16		
His 19	0.85	0.91	0.82		0.78	0.70	
Gln 20	0.83	0.87	0.78	0.34			
Arg 21	0.87	0.86	0.80	0.70	0.28		
Val 22	0.82	0.84	0.80	0.27, 0.25			
His 23	0.82	0.87	0.84		0.81	0.78	
Lys 24	0.79	0.77	0.74	0.64	0.49	0.19	
Asn 25	0.29	0.38	0.35				

[a] Order parameters were calculated from a 100-ps solvated MD trajectory using eq 10. As discussed in the caption to Table I, only the order parameters of the C–H1 spin pair of methylene groups have been reported.

Table III. Effective Internal Correlation Times for N–H and C–H Spin Pairs[a]

residue	NH	C^α	C^β	C^γ	C^δ	C^ϵ	C^ζ
Tyr 1	0.7	0.8	0.4		1.9	2.9	
Lys 2	0.3	2.0	7.0	7.0	4.0	3.1	
Cys 3	1.2	5.6	4.3				
Gly 4	4.6	5.8					
Leu 5	2.5	1.7	2.3	3.1	2.8, 3.6		
Cys 6	3.7	0.1	1.3				
Glu 7	1.1	3.1	2.9	2.9			
Arg 8	1.7	5.6	4.1	4.6	3.0		
Ser 9	2.5	1.8	2.1				
Phe 10	1.4	2.7	3.1		3.2	4.0	3.0
Val 11	3.6	7.9	4.3	7.1, 5.2			
Glu 12	4.2	5.1	3.9	5.9			
Lys 13	3.8	6.8	7.6	6.6	5.0	4.6	
Ser 14	3.6	3.6	0.2				
Ala 15	1.9	1.7	6.8				
Leu 16	3.0	3.6	2.7	2.5	5.9, 6.4		
Ser 17	3.0	4.2	2.7				
Arg 18	3.7	2.7	7.6	6.8	5.9		
His 19	3.7	4.0	3.7		2.5	3.0	
Gln 20	3.5	1.7	1.3	4.8			
Arg 21	0.6	4.7	3.6	5.4	6.1		
Val 22	4.1	4.9	3.6	5.6, 5.6			
His 23	1.5	5.2	3.2		1.0	1.7	
Lys 24	4.3	6.0	4.9	3.6	4.5	5.3	
Asn 25	6.3	6.0	5.8				

[a] All values are in picoseconds. Effective correlation times were determined from a 100-ps solvated MD simulation using eqs 4, 7, and 8. As discussed in the caption to Table I, only the effective correlation times for the C–H1 spin pairs of methylene groups have been reported; correlation times for C–H2 spin pairs were similar to the reported values.

from eqs 7 and 10 were consistent with the uncertainties in the order parameters estimated from eq 11. Generally, the order parameters were relatively large (>0.8) for the backbone C–H and N–H spin pairs and decreased montonically for C–H spin pairs along side chains. The terminal residues and the loop region (Val 11 to Lys 13) had lower than average order parameters for backbone spin pairs. Order parameters for Lys 2 and Arg 18 did not decrease montonically along the side chains; however, these trends were not statistically significant and were not observed in the second solvated MD simulation. The order parameters for the backbone N–H spin pairs were, on average, 0.06 unit smaller than the order parameters for the backbone C–H pairs; only for Gly 4 and Asn 25 were the order parameters significantly greater for the N–H pairs. While this result appears counterintuitive because the nitrogen atom is involved in the peptide bond, which has partial double bond character, similar conclusions have been inferred from experimental investigations of the ^{13}C relaxation of N-methyl amino acids in cyclosporin.[4] The effective internal correlation times (Table III) ranged from 0.2 to 7.0 ps and had a weak tendency to be longer for side C–H spin pairs than for backbone C–H and N–H spin pairs. Further interepretation of
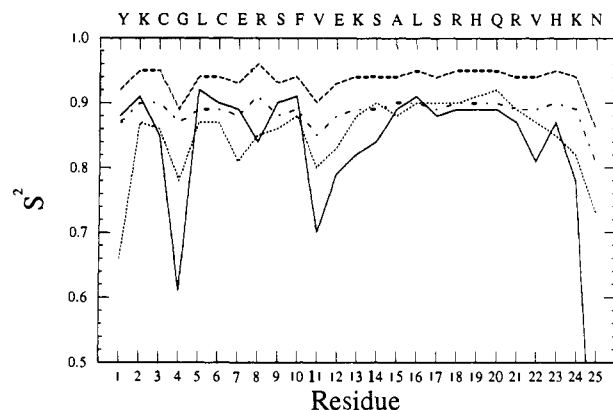
Figure 5. Order parameters for backbone C–H spin pairs. Shown are results for S^2 calculated from classical Langevin analysis (upper dashed curve), quantum Langevin analysis (lower dashed curve), vacuum MD simulation (dotted curve), and solvated MD simulation (solid curve).

the results presented in Table III is difficult because the effective correlation times are weighted averages (cf. eq 8) of the very fast (<1 ps) and slower (>1 ps) components of the correlation functions evident in Figure 3.

Graphs of the parameters for the Cα–H spin pairs determined by solvated and vacuum MD simulations and by classical and quantum mechanical Langevin calculations are shown in Figure 5. The trends in the order parameter along the backbone sequence of the peptide were similar for each calculation. Order parameters were generally high (>0.8) within elements of secondary structure and were reduced at the termini relative to the interior of the peptide. The order parameter for Gly 4 was reduced compared to the order parameters for flanking residues, and the loop region between Val 11 and Lys 13 had somewhat lower order parameters than either the β or helical elements of secondary structure. Overall, the order parameters for the classical Langevin analysis were greater than the order parameters for the quantum-mechanical Langevin analysis by approximately 0.05 unit; similar results were observed for N–H and side chain C–H spin pairs. This difference appears to arise primarily from zero-point motion in bending modes which is (necessarily) present in the quantum calculation but nearly absent in the classical analysis. Interestingly, the decrease in order parameter for Gly 4, compared with flanking residues, was less pronounced in the quantum-mechanical Langevin analysis than in the classical Langevin analysis or in the MD simulations. Both Langevin analyses gave higher order parameters, compared to the solvated MD simulation, for the loop and terminal regions of the peptide; similar results were observed for side chain C–H spin pairs. These results suggest, reasonably, that larger amplitude motions of the termini, loops, and side chains in the peptide are not adequately described as the superposition of small-amplitude damped harmonic motions.

Although the trends in order parameters for the vacuum and solvated MD simulations were similar for most backbone C–H spin pairs of the peptide, dramtic differences are observed for the two terminal residues. The order parameter for Tyr 1 was much less for the vacuum simulation than for the solvated simulation; the pattern was reversed for Asn 25. As discussed above, the hydrogen bonds between Tyr 1 and Phe 10 were not stable in the vacuum simulation; the increased mobility of the terminus that accompanies loss of the hydrogen bond was reflected in the lower order parameter in the vacuum simulation. Additionally, Asn 25 formed backbone and side chain hydrogen bonds in the simulation performed in vacuo that were not present in either the NMR starting structure or in the solvated MD simulation; the decreased mobility that accompanies formation of the hydrogen bonds accounted for the higher order parameter observed in the vacuum simulation. As one would hope for simulation performed with a realistic solvent description, the solution structures derived from the NMR data strongly support the hydrogen bond pattern seen in the solvated simulations and not that observed for the vacuum calculation.

Table IV. Experimental and Calculated Order Parameters for α C–H Spin Pairs[a]

residue	experiment	solvated MD	vacuum MD	Langevin	quantum Langevin
Tyr 1	0.74 ± 0.04	0.88	0.66	0.92	0.87
Lys 2	0.87 ± 0.04	0.91	0.87	0.95	0.90
Cys 3	0.88 ± 0.03	0.85	0.86	0.95	0.90
Gly 4[b]		0.61	0.78	0.89	0.87
Leu 5	0.88 ± 0.05	0.92	0.87	0.94	0.89
Cys 6	0.97 ± 0.05	0.90	0.87	0.94	0.89
Glu 7	0.85 ± 0.04	0.89	0.81	0.93	0.88
Arg 8	0.98 ± 0.09	0.84	0.85	0.96	0.91
Ser 9	0.86 ± 0.03	0.90	0.86	0.93	0.88
Phe 10	0.74 ± 0.03	0.91	0.88	0.94	0.89
Val 11	0.81 ± 0.03	0.70	0.80	0.90	0.85
Glu 12	0.79 ± 0.03	0.79	0.83	0.93	0.88
Lys 13	0.80 ± 0.03	0.82	0.88	0.94	0.89
Ser 14	0.82 ± 0.02	0.84	0.90	0.94	0.89
Ala 15	0.86 ± 0.04	0.89	0.88	0.94	0.90
Leu 16	0.88 ± 0.04	0.91	0.90	0.95	0.90
Ser 17	0.89 ± 0.03	0.88	0.90	0.94	0.89
Arg 18	0.88 ± 0.03	0.89	0.90	0.95	0.90
His 19	0.88 ± 0.04	0.89	0.91	0.95	0.90
Gln 20	0.84 ± 0.06	0.89	0.92	0.95	0.90
Arg 21	0.82 ± 0.03	0.87	0.89	0.94	0.89
Val 22	0.78 ± 0.04	0.81	0.87	0.94	0.89
His 23	0.74 ± 0.06	0.87	0.85	0.95	0.90
Lys 24	0.50 ± 0.02	0.78	0.82	0.94	0.89
Asn 25	0.30 ± 0.02	0.24	0.73	0.86	0.81

[a] Experimental values of the model-free order parameters, S_{MF}, were determined by analysis of NMR relaxation data using eq 6 and are taken from Table III of ref 7. Calculated order parameters were estimated using eq 7. The uncertainties in the order parameters calculated from the solvated and in vacuo MD simulations are estimated using eq 11 to be 0.04 and 0.02, respectively. [b] The order parameter was not measured experimentally for the Cα of Gly 4.
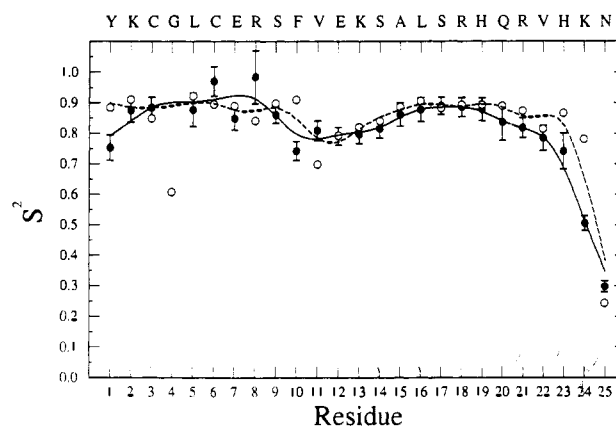

Figure 6. Comparison of experimental and theoretical order parameters. Experimental values and uncertainties in the order parameters for backbone α carbon spins are taken from ref 7 and shown as open circles; the solid line was drawn through these points using a three-point smoothing function. Similarly smoothed calculated values from the solvated MD simulation are shown with a dashed line. The order parameter for Gly 4 was not included when smoothing the data because it was not determined experimentally.

Order parameters and effective internal correlation times for the backbone α, Val β, Leu 5 γ, side chain methyl, and aromatic C–H spin pairs have been experimentally determined by NMR spectroscopy.[7,27] Comparisons of the experimental and theoretical order parameters are presented in Tables IV–VI; a graph of calculated and experimental order parameters is given in Figure 6. The solvated MD simulation reproduced the main features of the experimental results for the backbone C–H spin pairs, including the reduced order parameters for the loop region and the C-terminus. The main differences are that the order parameters of Tyr 1, Phe 10, and Lys 24 were higher in the simulation than the experiment. As discussed above, two hydrogen bonds exist between Tyr 1 and Phe 10 in the NMR structure and in the

Table V. Experimental and Calculated Order Parameters for Side Chain Methine and Aromatic C–H Spin Pairs[a]

residue	experiment	solvated MD	vacuum MD	Langevin	quantum Langevin
Tyr 1 C^δ	0.77 ± 0.03	0.71	0.43	0.86	0.84
Tyr 1 C^ϵ	0.71 ± 0.03	0.69	0.41	0.87	0.85
Leu 5 C^γ	0.48 ± 0.03	0.26	0.34	0.75	0.70
Phe 10 C^δ	0.79 ± 0.04	0.70	0.47	0.84	0.80
Phe 10 C^ϵ	0.95 ± 0.04	0.68	0.46	0.84	0.81
Phe 10 C^ζ	0.91 ± 0.04	0.75	0.71	0.88	0.83
Val 11 C^β	0.63 ± 0.03	0.74	0.79	0.87	0.82
Leu 16 C^{γ} [b]	0.99 ± 0.07	0.84	0.73	0.83	0.78
His 19 C^δ	0.86 ± 0.04	0.81	0.73	0.90	0.85
His 19 C^ϵ	0.90 ± 0.04	0.78	0.67	0.89	0.82
Val 22 C^β	0.55 ± 0.05	0.79	0.85	0.92	0.88
His 23 C^δ	0.78 ± 0.04	0.81	0.60	0.81	0.76
His 23 C^ϵ	0.73 ± 0.03	0.78	0.59	0.78	0.73

[a] Calculated order parameters were estimated from eq 7. Uncertainties in the order parameters for the solvated and in vacuo MD simulations are estimated to be respectively 0.06 and 0.03 using eq 11. Experimental values of the model-free order parameters were determined from NMR relaxation data using eq 6 and are taken from Table III of ref 7 and Table IV of ref 27. [b] The order parameter for Leu 16 C^γ could not be measured experimentally; instead the order parameter was estimated as the average order parameter measured for the two methyl C^δ C–H spin pairs divided by a factor of 0.1107 (eq 12).

Table VI. Experimental and Calculated Order Parameters for Methyl C–H Spin Pairs[a]

residue	experiment	solvated MD C–H	solvated MD C–C	vacuum MD C–H	vacuum MD C–C
Leu 5 C^δ	0.044 ± 0.003, 0.062 ± 0.004	0.38, 0.23	0.031, 0.028	0.12, 0.19	0.042, 0.042
Val 11 C^γ	0.063 ± 0.004, 0.091 ± 0.006	0.12, 0.38	0.072, 0.084	0.31, 0.58	0.084, 0.088
Ala 15 C^β	0.160 ± 0.010	0.57	0.100	0.74	0.101
Leu 16 C^δ	0.127 ± 0.008, 0.093 ± 0.006	0.24, 0.18	0.076, 0.076	0.38, 0.42	0.081, 0.083
Val 22 C^γ	0.069 ± 0.004, 0.086 ± 0.006	0.17, 0.18	0.072, 0.074	0.38, 0.28	0.086, 0.087

[a] Calculated order parameters for methyl C–H spin pairs were obtained directly from the correlation function for the C–H spin pairs using eq 7 (columns headed C–H) and indirectly from the correlation functions for the C–C symmetry axes of the methyl groups using eqs 7 and 12 (columns headed C–C). Experimental values were obtained by analysis of NMR relaxation data using eq 6 and are taken from Table V of ref 27.

solvated MD simulation; the experimental results suggest that the rigidity of these hydrogen bonds was overestimated in the simulation. The order parameters determined from experiment and from the solvated MD simulation for the side chain C–H spin pairs (Table V) agreed qualitatively. Good agreement was obtained for Tyr 1, Val 11, Leu 16, His 19, and His 23, but the simulation substantially overestimated the order parameters for Val 22 and underestimated them for Leu 5 and Phe 10. Detailed comparisons of experimental and theoretical values of the internal correlation times have not been attempted for reasons presented above and because experimental values could not be determined with sufficient precision.[7,27] However, the apparent experimental internal correlation times for many backbone and side chain methine carbons were greater than 20 ps, so that motions on timescales not sampled adequately in the present simulations may be important in determining NMR relaxation rates in solution and may account for the discrepancies between experimental and calculated order parameters for side chain C–H spin pairs.

The accuracy of correlation functions for the C–H spin pairs of methyl groups depends strongly on the degree to which transitions between rotomers are sampled during the simulation. Typically, only two–four transitions between rotomer positions occurred for each methyl group during the solvated simulations; between transitions, angular displacements within a rotomer had an rms magnitude of approximately 15°. As a consequence, nearly all of the order parameters determined directly from the correlation functions for C–H bond vectors were greater than the maximum theoretical value of 0.11 predicted by eq 12 and were also greater than the experimental values. For the same reasons, much better agreement was obtained using order parameters calculated indirectly from correlation functions for the C–C symmetry axes of the methyl groups using eq 12. The experimental value of the order parameter for the β methyl group of Ala 15 was significantly greater than 0.11, and significant differences were observed between order parameters for some of the geminal methyl groups (Val 11 and Leu 16 in particular). The order parameters calculated from the methyl symmetry axes using eq 12 do not reproduce the experimental differences between the order parameters for geminal methyl groups. As discussed elsewhere,[27] relatively show (>50–100 ps) motions may be important for NMR spin
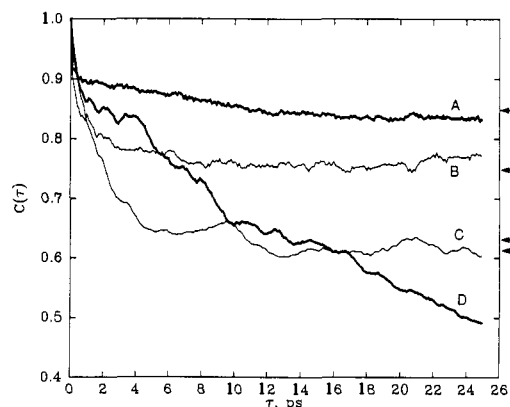

Figure 7. Correlation functions for selected H–H spin pairs. Values of the asymptotic order parameters calculated using eq 10 are indicated by arrows on the right-hand side of the graph, with curves A–D going from top to bottom: A, HN Arg 18 → NH His 19; B, Hβ2 Leu 5 → Hδ His 23; C, NHε Arg 8 → Hε His 19; D, NH Lys 12 → Hε Tyr 1.

Table VII. Values of S^2, R, and Q for Inter-Residue H–H Spin Pairs[a]

spin pairs	n	S^2	R	Q
backbone–backbone	68	0.78 ± 0.15	1.4 ± 0.7	0.98 ± 0.24
backbone–side chain	96	0.71 ± 0.16	1.8 ± 1.6	1.09 ± 0.40
sidechain–side chain	70	0.65 ± 0.18	2.2 ± 2.2	1.16 ± 0.44

[a] Order parameters were calculated from the 100-ps solvated MD simulation using eqs 4 and 7. The values of R and Q were calculated using eq 13. Values in the table give the mean and standard deviation for the distribution for n spin pairs of the types indicated.

relaxation of certain methyl ^{13}C spins, including the Ala 15 β carbon. The present simulations were too short to sample such motions.

C. H–H Spin Pairs. Correlation functions calculated from the 100-ps solvated MD trajectory using eq 4 are shown in Figure 7 for selected inter-residue H–H spin pairs. Their behavior was qualitatively similar to that for C–H and N–H spin pairs: a very rapid decay in the first few tenths of picoseconds was followed
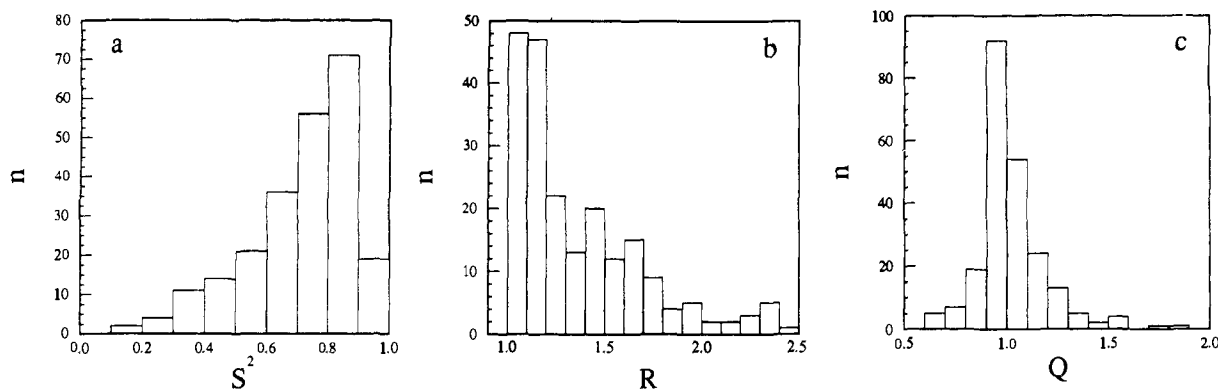
Figure 8. Distributions of S^2, R, and Q for 234 H–H spin pairs (see text). Twenty-six of the values for R were greater than 2.5 and are not shown in the graph; seven of the values for Q were greater than 2.0 and are not shown.

by a slower decay that generally reached an approximate plateau. Curve D is illustrative of a minor fraction of spin pairs whose correlation functions were strongly influenced by transitions that were poorly sampled during the time course of the present simulation. Statistics on the H–H behavior is given in Table VII for a set of 234 inter-residue pairs actually used in the NMR structure refinement. Spin pairs in which either of the spins is a methyl proton have been excluded from the reported results. Graphs of the corresponding distributions of S^2, R, and Q are given in Figure 8. The average values of S^2 decreased and the average values of R increased in proportion to the number of side chain protons present in the H–H spin pairs; the average values of Q tended to increase slightly. The widths of the distributions of all three quantities increased in proportion to the number of side chain spins. As shown in Figure 8, the distributions of S^2, R, and Q are skewed; 26 H–H spin pairs had values of $R > 2.5$ and 7 spin pairs had values of $Q > 2.0$. Three values of R were greater than 10, and two values of Q were larger than 3.5. In the absence of spin diffusion, apparent distances are proportional to the inverse sixth root of cross-peak intensities; these distributions imply that 97% of distance estimates obtained from the initial rates of development of NOESY cross-peaks would have relative errors of less than 12% due to neglect of internal motions; the remaining distance estimates would err by 12–25%. Comparable results for the distribution of Q have been obtained in simulations of lysozyme.[50] In actual practice, errors are probably less than these estimates since fixed distance calibrations (which are also affected by internal motion) are used. The essential point is that the distribution of Q is reasonably narrow.

Finally, Table VIII gives information relevant to the statistical uncertainties of the calculated order parameters. The difference between order parameters calculated at 20 ps and the asymptotic values had a mean less than 0.02 and a standard deviation of 0.04–0.06. Similarly low means but larger standard deviations (ranging from 0.08 for the backbone to 0.18 for side chains) were obtained from the comparison of independent simulations. Statistically, the standard deviations of the differences between order parameters determined by two independent simulations should be equal to the square root of the sum of the squares of the individual uncertainties (e.g., as estimated by eq 11 and reported in Table I). Thus, within the limitations imposed by the length of the simulations, the calculated order parameters were statistically well-behaved and did not appear to be systematically biased by the methods used to calculate order parameters from the trajectories. These conclusions apply primarily to the *distributions* illustrated in Figure 8 and Table VII; individual correlation functions, especially for side chains, may have poor reproducibility because of inefficient sampling of relatively rare events (see curve D in Figure 7).

IV. Discussion

As has been recognized for many years, NMR spectroscopy holds the promise of providing both structural and dynamical information about proteins at a high level of atomic detail. This recognition has been tempered by the realization that individual

Table VIII. Comparison of Order Parameters Calculated from Different Simulations[a]

comparison	spin pairs	$\langle \Delta S^2 \rangle$	σ	r
S^2 vs S_a^2	N–H and all C–H	0.02	0.06	0.96
	N–H and α C–H	0.01	0.04	0.96
	H–H	−0.01	0.06	0.95
duplicate simulations	N–H and all C–H	0.01	0.15	0.77
	N–H and α C–H	0.01	0.08	0.81
	H–H	−0.01	0.18	0.56

[a] Shown are the mean, $\langle \Delta S^2 \rangle$, and standard deviation, σ, of the distribution of differences between order parameters calculated using different methods. The first set of entries compares eq 7 to eq 10. The second set of entries compares order parameters estimated from two different solvated MD simulations. The spin pairs for which the comparisons are made are indicated in the second column of the table. Also shown are the linear correlation coefficients, r, for the comparisons.

measurements (such as a single cross-peak in a proton–proton NOESY spectrum) can be difficult to interpret since the spectral properties of a molecule depend upon both its average structure and its dynamical behavior. A promising way around this difficulty involves simultaneous analysis of a variety of experimental data (for protons and heavier nuclei) along with the use of theoretical models for the expected behavior of proteins in solution. The analysis reported here was driven by two advances in technology: the ability to measure ^{13}C relaxation parameters at natural abundance at many sites in a biomolecule[7] and improvements in computational methods that make solvated simulations of proteins accessible.

The solvated simulations reported here are in good agreement with experiment for two principal criteria. First, the "drift" of the structure away from that estimated from NMR data is acceptably small and is consistent with that seen in other protein simulations. All of the backbone hydrogen bonds found in the NMR structure are preserved in the simulations, and two independent simulations yielded distributions of order parameters essentially identical to within their expected uncertainties (cf. Table VIII). Second, order parameters computed for C–H spin pairs are in good agreement with experiment, although for some side chain positions, the statistical uncertainty in the simulation results makes this a weak comparison. Nevertheless, as Figure 6 shows, the general agreement of calculated and observed relaxation parameters along the backbone is quite good, suggesting that the simulations indeed reflect the molecular motions involved in these relaxation processes. The major limitation of the present results arises from the relatively short timescales (~ 100 ps) involved. While the short-time behavior seen in these calculations appears realistic, these results do not address the question of the importance of slower motions on NMR parameters. Simulations now in progress here and elsewhere will address this issue.

The normal mode calculations (either with or without consideration of the effects of solvent viscosity) show overall qualitative agreement with the molecular dynamics results, but the magnitude of the fluctuations about the average structure is smaller than in

the MD results (cf. Figure 5). The harmonic calculations do allow an estimate of quantum effects, and these appear to be nonnegligible for ^{13}C and ^{15}N relaxation: the order parameters arising from vibrations are about 0.05 lower when zero-point motion is considered than in a classical calculation. The behavior has been noted before[52] and will be important for precise comparisons of simulation with experiment. The vibrations responsible for this change appear to be mostly bending vibrations with frequencies in the 1000–1500-cm^{-1} range. Both solvated and vacuum dynamics indicate that the initial decay of $C(\tau)$ is oscillatory; in this respect the white-noise Langevin treatment appears to overstate the effects of viscous damping. It should be remembered, however, that NMR relaxation is insensitive to the details of atomic correlations on this timescale.

All the correlation functions show a rapid, vibrational contribution, followed by slower decay to a plateau value (cf. Figures 3 and 7). This has implications for the interepretation of internal correlation times determined from a model-free analysis of experimental data. Consider a reasonable but hypothetical case of $^{13}C\alpha$ relaxation in which the model-free analysis yields $S^2 = 0.85$ and $\tau_e = 50$ ps. About half the difference of S^2 from 1 is likely to arise from vibrational effects, with a very short time constant; the effective timescale for the remaining, slower motion (which is probably of greater physical interest) would then be 100 ps, since the model-free τ_e is essentially a weighted average of the vibrational and slower motion time constants (eq 8). Note that for side chain carbons, the initial fast decay can reduce S^2 to 0.8 or even less (cf. Figure 3). Detailed comparisons of τ_e values from experiment and simulation are made difficult at present by the limited precision with which they can be determined experimentally[7] and by the relatively short timescale of the present simulations, which precludes study of the nature of correlation functions in the 50–100-ps range (and longer).

The simulations reported here also are germane to the interpretation of proton NOESY cross-peaks in terms of distances for use in NMR structural refinements. Overall, the results are encouraging: the ratios of relaxation rate constants estimated from the full simulations to those that would be appropriate for a rigid molecule with the same average distance are distributed with a mean near 1 and a standard deviation of about 0.2–0.4 (Table VII, Figure 8); in addition, the fraction of proton NOESY peaks

for which the internal motion corrections are substantial is small, so a conservative application of distance constraints is appropriate. Hence, aside from methyl groups, neglect of the effects of internal motion should lead to relatively small errors in the derived distances. We and others have shown that relatively simple models for methyl motion that capture most of the essential physics can be incorporated into estimates of relaxation rate constants.[45,46]

Several limitations of this analysis of predicted proton NOESY intensities must be noted. First, the conclusions are based on relatively short simulations and may not include important contributions from longer processes. Second, the present results also apply directly only to a zinc-finger peptide, although the results are in general accord with simulations on larger proteins.[50,53,54] Third, complications arising from anisotropic rotational tumbling, which can systematically affect relaxation behavior, have not been considered.[55,56] Finally, correction factors given by eq 13 apply only to individual relaxation matrix *rate constants*; under many circumstances, multispin effects can make important contributions to observed cross-peak *intensities*, and systematic errors can arise from neglect of such multispin effects. This point has been extensively discussed in the recent literature, and a variety of methods are available to account for multispin effects.[57] The results presented here suggest that once the multispin complications are taken into account, the resulting distance estimates should be acceptably accurate for most structural studies.

(52) Brüschweiler, R. *J. Am. Chem. Soc.* 1992, *114*, 5341–5344.

(53) Chandrasekhar, I.; Clore, G. M.; Szabo, A.; Gronenborn, A. M.; Brooks, B. R. *J. Mol. Biol.* 1992, *226*, 239–250.
(54) Kördel, J.; Teleman, O. *J. Am. Chem. Soc.* 1992, *114*, 4934–4936.
(55) Duben, A. J.; Hutton, W. C. *J. Am. Chem. Soc.* 1990, *112*, 5917–5924.
(56) Withka, J. M.; Swaminathan, S.; Srinivasan, J.; Beveridge, D. L.; Bolton, P. H. *Science* 1992, *255*, 597–599.
(57) Borgias, B. A.; Gochin, M.; Kerwood, D. J.; James, T. L. *Prog. Nucl. Magn. Reson. Spectrosc.* 1990, *22*, 83–100.

Dynamic Behavior and Reactivity of (1,1,3,3-Tetramethylallyl)lithium

Jose Cabral and Gideon Fraenkel*

Contribution from the Department of Chemistry, The Ohio State University, Columbus, Ohio 43210. Received April 23, 1992

Abstract: (1,1,3,3-Tetramethylallyl)lithium (**1**), prepared by cleaving the corresponding phenyl sulfide **2** at −92 °C with lithium 1-(dimethylamino)naphthalenide or by reacting the trimethyltin derivative **3** with CH_3Li in THF/diethyl ether/TMEDA at −78 °C, adds rapidly to naphthalene and 1-(dimethylamino)naphthalene at −78 °C to give mixtures of the corresponding 1-substituted 1,2- and 1,4-dihydronaphthalenes. Carbon-13 NMR studies show **1**·TMEDA to be a contact ion-pair with Li^+-coordinated TMEDA disymmetrically sited with respect to the delocalized allyl counterion. Carbon-13 NMR line-shape analysis shows the barrier to allyl rotation $C_1C_2(C_2C_3)$ to be $\Delta H_r^* = 14$ kcal/mol with $\Delta S^* = 13$ eu. Analysis of the N–CH_3 ^{13}C NMR of contained TMEDA shows two dynamic processes take place, one a reorientation of coordinated Li^+ within the ion-pair (m) with $\Delta H_m^* = 7.9$ kcal/mol and $\Delta S_m^* = -5.3$ eu and the other the exhcange of TMEDA between its free and complexed states (bi) with $\Delta H_{bi}^* = 4.9$ kcal/mol and $\Delta S_{bi}^* = -29$ eu.

The influence of alkyl substituents on stability of π conjugated carbanions[1] is not well understood in part because few highly

alkylated carbanions have been prepared, let alone investigated.[2]

We recently described a convenient synthesis of (1,1,3,3-